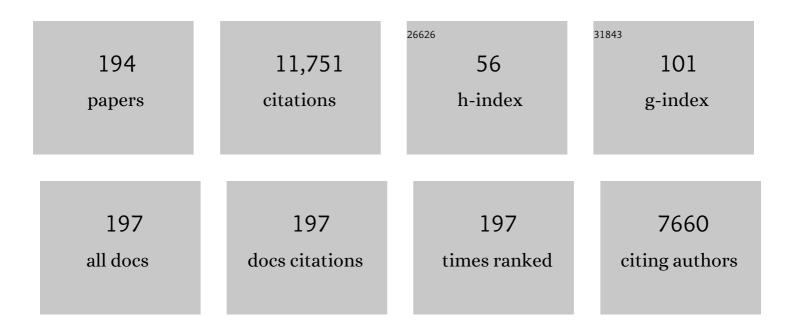
List of Publications by Year in descending order

Source: https://exaly.com/author-pdf/3879774/publications.pdf Version: 2024-02-01



#	Article	lF	CITATIONS
1	Niche differentiation of sulfur-oxidizing bacteria (SUP05) in submarine hydrothermal plumes. ISME Journal, 2022, 16, 1479-1490.	9.8	11
2	Spatial Variations in Magmatic Volatile Influx and Fluid Boiling in the Submarine Hydrothermal Systems of Niuatahi Caldera, Tonga Rearâ€Arc. Geochemistry, Geophysics, Geosystems, 2022, 23, .	2.5	5
3	Sulfur formation associated with coexisting sulfide minerals in the Kemp Caldera hydrothermal system, Scotia Sea. Chemical Geology, 2022, 606, 120927.	3.3	2
4	Hydrothermal activity and associated subsurface processes at Niuatahi rear-arc volcano, North East Lau Basin, SW Pacific: Implications from trace elements and stable isotope systematics in vent fluids. Geochimica Et Cosmochimica Acta, 2022, 332, 103-123.	3.9	5
5	The submarine Azores Plateau: Evidence for a waning mantle plume?. Marine Geology, 2022, 451, 106858.	2.1	5
6	Shallow-marine serpentinization-derived fluid seepage in the Upper Cretaceous Qahlah Formation, United Arab Emirates. Geological Magazine, 2021, 158, 1561-1571.	1.5	4
7	Podiform magnetite ore(s) in the Sabzevar ophiolite (NE Iran): oceanic hydrothermal alteration of a chromite deposit. Contributions To Mineralogy and Petrology, 2021, 176, 1.	3.1	3
8	Carbon isotopic composition of Frutexites in subseafloor ultramafic rocks. Biogeochemistry, 2021, 154, 525-536.	3.5	3
9	Serpentinization-Driven H2 Production From Continental Break-Up to Mid-Ocean Ridge Spreading: Unexpected High Rates at the West Iberia Margin. Frontiers in Earth Science, 2021, 9, .	1.8	15
10	Hydrothermal troctolite alteration at 300 and 400°C – Insights from flexible Au-reaction cell batch experimental investigations. American Mineralogist, 2021, , .	1.9	0
11	Effects of fluid boiling on Au and volatile element enrichment in submarine arc-related hydrothermal systems. Geochimica Et Cosmochimica Acta, 2021, 307, 105-132.	3.9	30
12	Massive cryptic microbe-sponge deposits in a Devonian fore-reef slope (Elbingerode Reef Complex, Harz) Tj ETQq	0 0 0 rgBT	Qverlock 2
13	SO2 disproportionation impacting hydrothermal sulfur cycling: Insights from multiple sulfur isotopes for hydrothermal fluids from the Tonga-Kermadec intraoceanic arc and the NE Lau Basin. Chemical Geology, 2021, 586, 120586.	3.3	15
14	Hydrogen Production from Alteration of Chicxulub Crater Impact Breccias: Potential Energy Source for a Subsurface Microbial Ecosystem. Astrobiology, 2021, 21, 1547-1564.	3.0	4
15	Formation of ethane and propane via abiotic reductive conversion of acetic acid in hydrothermal sediments. Proceedings of the National Academy of Sciences of the United States of America, 2021, 118, .	7.1	9
16	Trace Element and Isotope Systematics in Vent Fluids and Sulphides From Maka Volcano, North Eastern Lau Spreading Centre: Insights Into Three-Component Fluid Mixing. Frontiers in Earth Science, 2021, 9, .	1.8	6

17	On the controls of mineral assemblages and textures in alkaline springs, Samail Ophiolite, Oman. Chemical Geology, 2020, 533, 119435.	3.3	27
18	MARHYS (MARine HYdrothermal Solutions) Database: A Global Compilation of Marine Hydrothermal Vent Fluid, End Member, and Seawater Compositions. Geochemistry, Geophysics, Geosystems, 2020, 21, e2020GC009385.	2.5	30

#	Article	IF	CITATIONS
19	Isotope abundance ratio measurements using femtosecond laser ablation ionization mass spectrometry. Journal of Mass Spectrometry, 2020, 55, e4660.	1.6	10
20	Subcritical Phase Separation and Occurrence of Deep-Seated Brines at the NW Caldera Vent Field, Brothers Volcano: Evidence from Fluid Inclusions in Hydrothermal Precipitates. Geofluids, 2020, 2020, 1-22.	0.7	17
21	The convergence of minerals and life. Physics of Life Reviews, 2020, 34-35, 99-104.	2.8	1
22	Magmatic volatiles episodically flush oceanic hydrothermal systems as recorded by zoned epidote. Communications Earth & Environment, 2020, 1, .	6.8	9
23	Hydrogen generation and iron partitioning during experimental serpentinization of an olivine–pyroxene mixture. Geochimica Et Cosmochimica Acta, 2020, 282, 55-75.	3.9	30
24	Abiotic Sources of Molecular Hydrogen on Earth. Elements, 2020, 16, 19-24.	0.5	62
25	Crystal surface reactivity analysis using a combined approach of X-ray micro-computed tomography and vertical scanning interferometry. Numerische Mathematik, 2020, 320, 27-52.	1.4	11
26	Mineral self-organization on a lifeless planet. Physics of Life Reviews, 2020, 34-35, 62-82.	2.8	28
27	Variant across-forearc compositions of slab-fluids recorded by serpentinites: Implications on the mobilization of FMEs from an active subduction zone (Mariana forearc). Lithos, 2020, 364-365, 105525.	1.4	9
28	Complex subsurface hydrothermal fluid mixing at a submarine arc volcano supports distinct and highly diverse microbial communities. Proceedings of the National Academy of Sciences of the United States of America, 2020, 117, 32627-32638.	7.1	36
29	Fluid–rock interactions in the shallow Mariana forearc: carbon cycling and redox conditions. Solid Earth, 2019, 10, 907-930.	2.8	16
30	Geochemistry and mineralogy of serpentinization-driven hyperalkaline springs in the Ronda peridotites. Lithos, 2019, 350-351, 105215.	1.4	15
31	Application of B, Mg, Li, and Sr Isotopes in Acidâ€Sulfate Vent Fluids and Volcanic Rocks as Tracers for Fluidâ€Rock Interaction in Backâ€Arc Hydrothermal Systems. Geochemistry, Geophysics, Geosystems, 2019, 20, 5849-5866.	2.5	8
32	Biodegradability of hydrothermally altered deep-sea dissolved organic matter. Marine Chemistry, 2019, 217, 103706.	2.3	6
33	Carbon cycling in low temperature hydrothermal systems: The Dorado Outcrop. Geochimica Et Cosmochimica Acta, 2019, 264, 1-12.	3.9	9
34	Geochemical characterization of highly diverse hydrothermal fluids from volcanic vent systems of the Kermadec intraoceanic arc. Chemical Geology, 2019, 528, 119289.	3.3	38
35	The behavior of trace elements in seawater, sedimentary pore water, and their incorporation into carbonate minerals: a review. Facies, 2019, 65, 1.	1.4	109
36	Evidence for Lowâ€Temperature Diffuse Venting at North Pond, Western Flank of the Midâ€Atlantic Ridge. Geochemistry, Geophysics, Geosystems, 2019, 20, 2572-2584.	2.5	6

#	Article	IF	CITATIONS
37	Extreme intensity of fluid-rock interaction during extensive intraplate volcanism. Geochimica Et Cosmochimica Acta, 2019, 257, 26-48.	3.9	6
38	Geochemistry of hot-springs at the SuSu Knolls hydrothermal field, Eastern Manus Basin: Advanced argillic alteration and vent fluid acidity. Geochimica Et Cosmochimica Acta, 2019, 255, 25-48.	3.9	27
39	Parameters Governing the Community Structure and Element Turnover in Kermadec Volcanic Ash and Hydrothermal Fluids as Monitored by Inorganic Electron Donor Consumption, Autotrophic CO2 Fixation and 16S Tags of the Transcriptome in Incubation Experiments. Frontiers in Microbiology, 2019, 10. 2296.	3.5	14
40	Microbial metalâ€sulfide oxidation in inactive hydrothermal vent chimneys suggested by metagenomic and metaproteomic analyses. Environmental Microbiology, 2019, 21, 682-701.	3.8	50
41	Quartz veins with associated Sb-Pb-Ag±Au mineralization in the Schwarzwald, SW Germany: a record of metamorphic cooling, tectonic rifting, and element remobilization processes in the Variscan belt. Mineralium Deposita, 2019, 54, 281-306.	4.1	13
42	Geology and Fluid Discharge at Dorado Outcrop, a Low Temperature Ridgeâ€Flank Hydrothermal System. Geochemistry, Geophysics, Geosystems, 2019, 20, 487-504.	2.5	18
43	Melt Impregnation of Mantle Peridotite Facilitates Highâ€Temperature Hydration and Mechanical Weakening: Implications for Oceanic Detachment Faults. Geochemistry, Geophysics, Geosystems, 2019, 20, 84-108.	2.5	6
44	Genesis of hydrothermal silver-antimony-sulfide veins of the BrÃ ¤ nsdorf sector as part of the classic Freiberg silver mining district, Germany. Mineralium Deposita, 2019, 54, 263-280.	4.1	20
45	Biological methane production under putative Enceladus-like conditions. Nature Communications, 2018, 9, 748.	12.8	91
46	Constraints on the source of Cu in a submarine magmatic-hydrothermal system, Brothers volcano, Kermadec island arc. Contributions To Mineralogy and Petrology, 2018, 173, 1.	3.1	29
47	Sulfidation of major rock types of the oceanic lithosphere; An experimental study at 250 °C and 400 bars. Lithos, 2018, 323, 208-217.	1.4	3
48	The influence of magmatic fluids and phase separation on B systematics in submarine hydrothermal vent fluids from back-arc basins. Geochimica Et Cosmochimica Acta, 2018, 232, 140-162.	3.9	12
49	Evidence for archaeal methanogenesis within veins at the onshore serpentinite-hosted Chimaera seeps, Turkey. Chemical Geology, 2018, 483, 567-580.	3.3	27
50	Fossilized Life in Subseafloor Ultramafic Rocks. Geomicrobiology Journal, 2018, 35, 460-467.	2.0	11
51	Anaerobic methane oxidation inducing carbonate precipitation at abiogenic methane seeps in the Tuscan archipelago (Italy). PLoS ONE, 2018, 13, e0207305.	2.5	21
52	Constraints on Cooling of the Lower Ocean Crust From Epidote Veins in the Wadi Gideah Section, Oman Ophiolite. Geochemistry, Geophysics, Geosystems, 2018, 19, 4195-4217.	2.5	9
53	Simulating putative Enceladus-like conditions: The possibility of biological methane production on Saturn's icy moon. Proceedings of the International Astronomical Union, 2018, 14, 219-221.	0.0	1
54	Metaproteogenomic Profiling of Microbial Communities Colonizing Actively Venting Hydrothermal Chimneys. Frontiers in Microbiology, 2018, 9, 680.	3.5	36

#	Article	IF	CITATIONS
55	Magma plumbing and hybrid magma formation at an active back-arc basin volcano: North Su, eastern Manus basin. Journal of Volcanology and Geothermal Research, 2018, 362, 1-16.	2.1	7
56	Cretaceous seawater and hydrothermal fluid compositions recorded in abiogenic carbonates from the Troodos Ophiolite, Cyprus. Chemical Geology, 2018, 494, 43-55.	3.3	9
57	Comparing biosignatures in aged basalt glass from North Pond, Mid-Atlantic Ridge and the Louisville Seamount Trail, off New Zealand. PLoS ONE, 2018, 13, e0190053.	2.5	3
58	Hydrothermal Vents. Encyclopedia of Earth Sciences Series, 2018, , 711-715.	0.1	0
59	Time-resolved interaction of seawater with gabbro: An experimental study of rare-earth element behavior up to 475 °C, 100 MPa. Geochimica Et Cosmochimica Acta, 2017, 197, 167-192.	3.9	8
60	The Cogne magnetite deposit (Western Alps, Italy): A Late Jurassic seafloor ultramafic-hosted hydrothermal system?. Ore Geology Reviews, 2017, 83, 103-126.	2.7	17
61	Niche partitioning of diverse sulfur-oxidizing bacteria at hydrothermal vents. ISME Journal, 2017, 11, 1545-1558.	9.8	168
62	New insight on Li and B isotope fractionation during serpentinization derived from batch reaction investigations. Geochimica Et Cosmochimica Acta, 2017, 217, 51-79.	3.9	17
63	Reaction-induced porosity and onset of low-temperature carbonation in abyssal peridotites: Insights from 3D high-resolution microtomography. Lithos, 2017, 268-271, 274-284.	1.4	23
64	A new X-ray-transparent flow-through reaction cell for a <i>μ</i> -CT-based concomitant surveillance of the reaction progress of hydrothermal mineral–fluid interactions. Solid Earth, 2016, 7, 651-658.	2.8	5
65	Some Compositional and Kinetic Controls on the Bioenergetic Landscapes in Oceanic Basement. Frontiers in Microbiology, 2016, 7, 107.	3.5	44
66	Nitrogen Stimulates the Growth of Subsurface Basalt-associated Microorganisms at the Western Flank of the Mid-Atlantic Ridge. Frontiers in Microbiology, 2016, 7, 633.	3.5	19
67	Iron Transformation Pathways and Redox Micro-Environments in Seafloor Sulfide-Mineral Deposits: Spatially Resolved Fe XAS and Î'57/54Fe Observations. Frontiers in Microbiology, 2016, 7, 648.	3.5	20
68	Hydrothermalism. Encyclopedia of Earth Sciences Series, 2016, , 344-357.	0.1	5
69	Serpentinization. Encyclopedia of Earth Sciences Series, 2016, , 779-787.	0.1	1
70	Molecular alteration of marine dissolved organic matter under experimental hydrothermal conditions. Geochimica Et Cosmochimica Acta, 2016, 175, 68-85.	3.9	73
71	Temperature trends for reaction rates, hydrogen generation, and partitioning of iron during experimental serpentinization of olivine. Geochimica Et Cosmochimica Acta, 2016, 181, 175-200.	3.9	143
72	Arsenic bioaccumulation and biotransformation in deep-sea hydrothermal vent organisms from the PACMANUS hydrothermal field, Manus Basin, PNG. Deep-Sea Research Part I: Oceanographic Research Papers, 2016, 117, 95-106.	1.4	10

#	Article	IF	CITATIONS
73	Establishing criteria to distinguish oil-seep from methane-seep carbonates. Geology, 2016, 44, 667-670.	4.4	35
74	Heterotrophic <i>Proteobacteria</i> in the vicinity of diffuse hydrothermal venting. Environmental Microbiology, 2016, 18, 4348-4368.	3.8	63
75	Subaqueous cryptodome eruption, hydrothermal activity and related seafloor morphologies on the andesitic North Su volcano. Journal of Volcanology and Geothermal Research, 2016, 323, 80-96.	2.1	11
76	Hydrothermal Vents. Encyclopedia of Earth Sciences Series, 2016, , 1-5.	0.1	0
77	Uâ€Pb dating of interspersed gabbroic magmatism and hydrothermal metamorphism during lower crustal accretion, Vema lithospheric section, Midâ€Atlantic Ridge. Journal of Geophysical Research: Solid Earth, 2015, 120, 2093-2118.	3.4	11
78	Zygomycetes in Vesicular Basanites from Vesteris Seamount, Greenland Basin – A New Type of Cryptoendolithic Fungi. PLoS ONE, 2015, 10, e0133368.	2.5	21
79	Fluid circulation and carbonate vein precipitation in the footwall of an oceanic core complex, <scp>O</scp> cean <scp>D</scp> rilling <scp>P</scp> rogram <scp>S</scp> ite 175, <scp>M</scp> idâ€ <scp>A</scp> tlantic <scp>R</scp> idge. Geochemistry, Geophysics, Geosystems, 2015, 16, 3716-3732.	2.5	19
80	Palagonitization of Basalt Glass in the Flanks of Mid-Ocean Ridges: Implications for the Bioenergetics of Oceanic Intracrustal Ecosystems. Astrobiology, 2015, 15, 793-803.	3.0	15
81	Rare earth element evolution and migration in plagiogranites: a record preserved in epidote and allanite of the Troodos ophiolite. Contributions To Mineralogy and Petrology, 2015, 169, 1.	3.1	28
82	Origin of Silicic Magmas at Spreading Centres—an Example from the South East Rift, Manus Basin. Journal of Petrology, 2015, 56, 255-272.	2.8	29
83	Submarine venting of magmatic volatiles in the Eastern Manus Basin, Papua New Guinea. Geochimica Et Cosmochimica Acta, 2015, 163, 178-199.	3.9	59
84	Ultramafic clasts from the South Chamorro serpentine mud volcano reveal a polyphase serpentinization history of the Mariana forearc mantle. Lithos, 2015, 227, 1-20.	1.4	31
85	Efficient removal of recalcitrant deep-ocean dissolved organic matter during hydrothermalÂcirculation. Nature Geoscience, 2015, 8, 856-860.	12.9	104
86	Hydrothermalism. , 2015, , 1-20.		0
87	Hydrogeologic Properties, Processes, and Alteration in the Igneous Ocean Crust. Developments in Marine Geology, 2014, , 507-551.	0.4	9
88	Serpentinization. , 2014, , 1-12.		0
89	Microbial lipids reveal carbon assimilation patterns on hydrothermal sulfide chimneys. Environmental Microbiology, 2014, 16, 3515-3532.	3.8	44
90	Magnetite in seafloor serpentiniteSome like it hot. Geology, 2014, 42, 135-138.	4.4	192

#	Article	IF	CITATIONS
91	Effects of temperature, sulfur, and oxygen fugacity on the composition of sphalerite from submarine hydrothermal vents. Geology, 2014, 42, 699-702.	4.4	143
92	Garnets within geode-like serpentinite veins: Implications for element transport, hydrogen production and life-supporting environment formation. Geochimica Et Cosmochimica Acta, 2014, 141, 454-471.	3.9	40
93	Geologic setting of PACManus hydrothermal area — High resolution mapping and in situ observations. Marine Geology, 2014, 355, 98-114.	2.1	27
94	Mineralogy Drives Bacterial Biogeography of Hydrothermally Inactive Seafloor Sulfide Deposits. Geomicrobiology Journal, 2013, 30, 313-326.	2.0	52
95	Oxygen consumption rates in subseafloor basaltic crust derived from a reaction transport model. Nature Communications, 2013, 4, 2539.	12.8	96
96	An Early Jurassic brachiopod-dominated seep deposit enclosed by serpentinite, eastern Oregon, USA. Palaeogeography, Palaeoclimatology, Palaeoecology, 2013, 390, 4-16.	2.3	25
97	Calcium carbonate veins in ocean crust record a threefold increase of seawater Mg/Ca in the past 30 million years. Earth and Planetary Science Letters, 2013, 362, 215-224.	4.4	66
98	The oxygen isotope equilibrium fractionation between sulfite species and water. Geochimica Et Cosmochimica Acta, 2013, 120, 562-581.	3.9	41
99	Compositional controls on hydrogen generation during serpentinization of ultramafic rocks. Lithos, 2013, 178, 55-69.	1.4	202
100	Metasomatism Within the Ocean Crust. Lecture Notes in Earth System Sciences, 2013, , 253-288.	0.6	26
101	The influence of bacterial activity on phosphorite formation in the Miocene Monterey Formation, California. Palaeogeography, Palaeoclimatology, Palaeoecology, 2012, 317-318, 171-181.	2.3	31
102	Interstitial fluid chemistry of sediments underlying the North Atlantic gyre and the influence of subsurface fluid flow. Earth and Planetary Science Letters, 2012, 323-324, 79-91.	4.4	77
103	Geochemically induced shifts in catabolic energy yields explain past ecological changes of diffuse vents in the East Pacific Rise 9°50'N area. Geochemical Transactions, 2012, 13, 2.	0.7	13
104	Geochemistry of hydrothermal fluids from the PACMANUS, Northeast Pual and Vienna Woods hydrothermal fields, Manus Basin, Papua New Guinea. Geochimica Et Cosmochimica Acta, 2011, 75, 1088-1123.	3.9	185
105	Catabolic and anabolic energy for chemolithoautotrophs in deep-sea hydrothermal systems hosted in different rock types. Geochimica Et Cosmochimica Acta, 2011, 75, 5736-5748.	3.9	199
106	Dehydration of subducting serpentinite: Implications for halogen mobility in subduction zones and the deep halogen cycle. Earth and Planetary Science Letters, 2011, 308, 65-76.	4.4	176
107	Carbonate veins trace seawater circulation during exhumation and uplift of mantle rock: Results from ODP Leg 209. Earth and Planetary Science Letters, 2011, 311, 242-252.	4.4	51
108	Geochemistry of vent fluid particles formed during initial hydrothermal fluid-seawater mixing along the Mid-Atlantic Ridge. Geochemistry, Geophysics, Geosystems, 2011, 12, n/a-n/a.	2.5	26

#	Article	IF	CITATIONS
109	Driving forces behind the biotope structures in two low-temperature hydrothermal venting sites on the southern Mid-Atlantic Ridge. Environmental Microbiology Reports, 2011, 3, 727-737.	2.4	25
110	Colonization of subsurface microbial observatories deployed in young ocean crust. ISME Journal, 2011, 5, 692-703.	9.8	155
111	Ultra-diffuse hydrothermal venting supports Fe-oxidizing bacteria and massive umber deposition at 5000 m off Hawaii. ISME Journal, 2011, 5, 1748-1758.	9.8	97
112	Hydrogen is an energy source for hydrothermal vent symbioses. Nature, 2011, 476, 176-180.	27.8	251
113	Tapping the Subsurface Ocean Crust Biosphere: Low Biomass and Drilling-Related Contamination Calls for Improved Quality Controls. Geomicrobiology Journal, 2010, 27, 158-169.	2.0	54
114	Future Scientific Drilling of Oceanic Crust. Eos, 2010, 91, 133.	0.1	1
115	Alteration of the Oceanic Lithosphere and Implications for Seafloor Processes. Elements, 2010, 6, 173-178.	0.5	74
116	Rare earth element abundances in hydrothermal fluids from the Manus Basin, Papua New Guinea: Indicators of sub-seafloor hydrothermal processes in back-arc basins. Geochimica Et Cosmochimica Acta, 2010, 74, 5494-5513.	3.9	137
117	Insights to magmatic–hydrothermal processes in the Manus back-arc basin as recorded by anhydrite. Geochimica Et Cosmochimica Acta, 2010, 74, 5514-5536.	3.9	44
118	Magmatic influence on reaction paths and element transport during serpentinization. Chemical Geology, 2010, 274, 196-211.	3.3	42
119	Rare earth elements in authigenic methane-seep carbonates as tracers for fluid composition during early diagenesis. Chemical Geology, 2010, 277, 126-136.	3.3	129
120	The petrology of seafloor rodingites: Insights from geochemical reaction path modeling. Lithos, 2009, 112, 103-117.	1.4	131
121	Stable isotope (δ180, δD, δ37Cl) evidence for multiple fluid histories in mid-Atlantic abyssal peridotites (ODP Leg 209). Lithos, 2009, 110, 83-94.	1.4	68
122	Formation and alteration of plagiogranites in an ultramafic-hosted detachment fault at the Mid-Atlantic Ridge (ODP Leg 209). Contributions To Mineralogy and Petrology, 2009, 157, 625-639.	3.1	46
123	The diversity and abundance of bacteria inhabiting seafloor lavas positively correlate with rock alteration. Environmental Microbiology, 2009, 11, 86-98.	3.8	100
124	Shortâ€ŧerm microbial and physicoâ€chemical variability in lowâ€ŧemperature hydrothermal fluids near 5°S on the Midâ€Atlantic Ridge. Environmental Microbiology, 2009, 11, 2526-2541.	3.8	44
125	Serpentinized troctolites exposed near the Kairei Hydrothermal Field, Central Indian Ridge: Insights into the origin of the Kairei hydrothermal fluid supporting a unique microbial ecosystem. Earth and Planetary Science Letters, 2009, 280, 128-136.	4.4	86
126	Geochemical constraints on the modes of carbonate precipitation in peridotites from the Logatchev Hydrothermal Vent Field and Gakkel Ridge. Chemical Geology, 2009, 268, 97-106.	3.3	36

WOLFGANG BACH

#	Article	IF	CITATIONS
127	Biogenic iron oxyhydroxide formation at mid-ocean ridge hydrothermal vents: Juan de Fuca Ridge. Geochimica Et Cosmochimica Acta, 2009, 73, 388-403.	3.9	150
128	Thermodynamic constraints on hydrogen generation during serpentinization of ultramafic rocks. Geochimica Et Cosmochimica Acta, 2009, 73, 856-875.	3.9	415
129	lron partitioning and hydrogen generation during serpentinization of abyssal peridotites from 15°N on the Mid-Atlantic Ridge. Geochimica Et Cosmochimica Acta, 2009, 73, 6868-6893.	3.9	269
130	Evidence for cryptoendolithic life in Devonian pillow basalts of Variscan orogens, Germany. Palaeogeography, Palaeoclimatology, Palaeoecology, 2009, 283, 120-125.	2.3	32
131	δ37Cl systematics of a backarc spreading system: The Lau Basin. Geology, 2009, 37, 427-430.	4.4	47
132	Fe-Ni-Co-O-S Phase Relations in Peridotite-Seawater Interactions. Journal of Petrology, 2009, 50, 37-59.	2.8	212
133	Authigenesis of Carbonate Minerals in Modern and Devonian Oceanâ€Floor Hard Rocks. Journal of Geology, 2009, 117, 307-323.	1.4	24
134	Abundance and diversity of microbial life in ocean crust. Nature, 2008, 453, 653-656.	27.8	339
135	Putative cryptoendolithic life in Devonian pillow basalt, Rheinisches Schiefergebirge, Germany. Geobiology, 2008, 6, 125-135.	2.4	56
136	Calcium isotope (δ44/40Ca) fractionation along hydrothermal pathways, Logatchev field (Mid-Atlantic) Tj ETQq0 (0	Overlock 10
137	Integrated Fe- and S-isotope study of seafloor hydrothermal vents at East Pacific Rise 9–10°N. Chemical Geology, 2008, 252, 214-227.	3.3	199
138	Sulfur isotope measurement of sulfate and sulfide by high-resolution MC-ICP-MS. Chemical Geology, 2008, 253, 102-113.	3.3	143
139	Hydrothermal alteration and microbial sulfate reduction in peridotite and gabbro exposed by detachment faulting at the Midâ€Atlantic Ridge, 15°20′N (ODP Leg 209): A sulfur and oxygen isotope study. Geochemistry, Geophysics, Geosystems, 2007, 8, .	2.5	123
140	A Simplified, Accurate and Fast Method for Lithium Isotope Analysis of Rocks and Fluids, and ?7Li Values of Seawater and Rock Reference Materials. Geostandards and Geoanalytical Research, 2007, 31, 77-88.	1.9	73
141	Biological formation of ethane and propane in the deep marine subsurface. Proceedings of the National Academy of Sciences of the United States of America, 2006, 103, 14684-14689.	7.1	235
142	Energy in the dark: Fuel for life in the deep ocean and beyond. Eos, 2006, 87, 73.	0.1	23

#	Article	IF	CITATIONS
145	Unraveling the sequence of serpentinization reactions: petrography, mineral chemistry, and petrophysics of serpentinites from MAR 15°N (ODP Leg 209, Site 1274). Geophysical Research Letters, 2006, 33, .	4.0	311
146	Phyllosilicate Alteration Mineral Assemblages in the Active Subsea-Floor Pacmanus Hydrothermal System, Papua New Guinea, ODP Leg 193. Economic Geology, 2006, 101, 633-650.	3.8	21
147	On the Sr isotope and REE compositions of anhydrites from the TAG seafloor hydrothermal system. Geochimica Et Cosmochimica Acta, 2005, 69, 1511-1525.	3.9	43
148	Heating and freezing experiments on aqueous fluid inclusions in anhydrite: Recognition and effects of stretching and the low-temperature formation of gypsum. Chemical Geology, 2005, 223, 35-45.	3.3	16
149	Geomicrobiology in oceanography: microbe–mineral interactions at and below the seafloor. Trends in Microbiology, 2005, 13, 449-456.	7.7	245
150	87Sr/86Sr, 3He/4He, REE and stable isotope (δ34S, δ18O) constraints on the hydrothermal fluid evolution of the PACMANUS system, Manus Basin. , 2005, , 813-815.		0
151	Fluid flow and fluid-rock interaction within ocean crust: Reconciling geochemical, geological, and geophysical observations. Geophysical Monograph Series, 2004, , 99-117.	0.1	8
152	Fluid inclusion evidence for subsurface phase separation and variable fluid mixing regimes beneath the deep-sea PACMANUS hydrothermal field, Manus Basin back arc rift, Papua New Guinea. Journal of Geophysical Research, 2004, 109, .	3.3	32
153	Seawater-peridotite interactions: First insights from ODP Leg 209, MAR 15°N. Geochemistry, Geophysics, Geosystems, 2004, 5, n/a-n/a.	2.5	281
154	Neutrophilic Iron-Oxidizing Bacteria in the Ocean: Their Habitats, Diversity, and Roles in Mineral Deposition, Rock Alteration, and Biomass Production in the Deep-Sea. Geomicrobiology Journal, 2004, 21, 393-404.	2.0	159
155	Secondary ion mass spectrometry for the determination of δ37Cl. Chemical Geology, 2004, 207, 277-289.	3.3	30
156	Hydrothermal venting in magma deserts: The ultraslow-spreading Gakkel and Southwest Indian Ridges. Geochemistry, Geophysics, Geosystems, 2004, 5, .	2.5	93
157	Contrasting evolution of hydrothermal fluids in the PACMANUS system, Manus Basin: The Sr and S isotope evidence. Geology, 2003, 31, 805.	4.4	40
158	Controls of fluid chemistry and complexation on rare-earth element contents of anhydrite from the Pacmanus subseafloor hydrothermal system, Manus Basin, Papua New Guinea. Mineralium Deposita, 2003, 38, 916-935.	4.1	77
159	Rhenium-osmium isotope systematics and platinum group element concentrations in oceanic crust from DSDP/ODP Sites 504 and 417/418. Geochemistry, Geophysics, Geosystems, 2003, 4, .	2.5	80
160	Geochemistry of hydrothermally altered oceanic crust: DSDP/ODP Hole 504B - Implications for seawater-crust exchange budgets and Sr- and Pb-isotopic evolution of the mantle. Geochemistry, Geophysics, Geosystems, 2003, 4, .	2.5	143
161	Geomicrobiology of the Ocean Crust: A Role for Chemoautotrophic Fe-Bacteria. Biological Bulletin, 2003, 204, 180-185.	1.8	62
162	Iron and sulfide oxidation within the basaltic ocean crust: implications for chemolithoautotrophic microbial biomass production. Geochimica Et Cosmochimica Acta, 2003, 67, 3871-3887.	3.9	345

#	Article	IF	CITATIONS
163	Discovery of ancient and active hydrothermal systems along the ultra-slow spreading Southwest Indian Ridge 10°-16°E. Geochemistry, Geophysics, Geosystems, 2002, 3, 1-14.	2.5	110
164	Sr isotope variations in vent fluids from 9°46â€2-9°54â€2N East Pacific Rise: evidence of a non-zero-Mg fluid component. Geochimica Et Cosmochimica Acta, 2001, 65, 729-739.	3.9	27
165	The geochemical consequences of late-stage low-grade alteration of lower ocean crust at the SW Indian Ridge: results from ODP Hole 735B (Leg 176). Geochimica Et Cosmochimica Acta, 2001, 65, 3267-3287.	3.9	159
166	A long in situ section of the lower ocean crust: results of ODP Leg 176 drilling at the Southwest Indian Ridge. Earth and Planetary Science Letters, 2000, 179, 31-51.	4.4	456
167	Relationship between the Sr and O isotope compositions of hydrothermal fluids and the spreading and magma-supply rates at oceanic spreading centers. Geology, 1999, 27, 1067.	4.4	60
168	A helium, argon, and nitrogen record of the upper continental crust (KTB drill holes, Oberpfalz,) Tj ETQq0 0 0 rgB1	- /Qyerlock	10 Tf 50 54
169	Rare earth element mobility in the oceanic lower sheeted dyke complex: evidence from geochemical data and leaching experiments. Chemical Geology, 1998, 151, 309-326.	3.3	56
170	Atmospheric noble gases in volcanic glasses from the southern Lau Basin: origin from the subducting slab?. Earth and Planetary Science Letters, 1998, 160, 297-309.	4.4	37
171	Anomalously nucleogenic neon in North Chile Ridge basalt glasses suggesting a previously degassed mantle source. Earth and Planetary Science Letters, 1998, 160, 447-462.	4.4	27
172	Chemical fluxes in the Tonga Subduction Zone: Evidence from the Southern Lau Basin. Geophysical Research Letters, 1998, 25, 1467-1470.	4.0	28
173	Noble gas evidence for a lower mantle component in MORBs from the southern East Pacific Rise: Decoupling of helium and neon isotope systematics. Geochimica Et Cosmochimica Acta, 1997, 61, 2697-2715.	3.9	167
174	Paleofluids and Recent fluids in the upper continental crust: Results from the German Continental Deep Drilling Program (KTB). Journal of Geophysical Research, 1997, 102, 18233-18254.	3.3	117
175	Unusually large NbTa depletions in North Chile ridge basalts at 36°50′ to 38°56′S: major element, trace element, and isotopic data. Earth and Planetary Science Letters, 1996, 142, 223-240.	4.4	60
176	Chemical remanent magnetization in oceanic sheeted dikes. Geophysical Research Letters, 1996, 23, 1123-1126.	4.0	5
177	New evidence for the production of EM-type ocean island basalts and large volumes of volcaniclastites during the early history of the Manihiki Plateau. Marine Geology, 1995, 122, 181-205.	2.1	18
178	Chemical and isotopic variations along the superfast spreading East Pacific Rise from 6 to 30�S. Contributions To Mineralogy and Petrology, 1994, 116, 365-380.	3.1	113
179	Design and deployment of borehole observatories and experiments during IODP Expedition 336, Mid-Atlantic Ridge flank at North Pond. Proceedings of the Integrated Ocean Drilling Program Integrated Ocean Drilling Program, 0, , .	1.0	21
180	Volatile Components in Basalts and Basaltic Glasses from the EPR at $9 \hat{A}^o 30' N.$, 0, , .		2

#	Article	IF	CITATIONS
181	Chemistry of the Lower Sheeted Dike Complex, Hole 504B (Leg 148): Influence of Magmatic Differentiation and Hydrothermal Alteration. , 0, , .		14
182	Stable and Strontium Isotopic Profiles through Hydrothermally Altered Upper Oceanic Crust, Hole 504B. , 0, , .		15
183	Ridge-Flank Alteration of Upper Ocean Crust in the Eastern Pacific: Synthesis of Results for Volcanic Rocks of Holes 504B and 896A. , 0, , .		23
184	Hydrothermal Alteration of a Section of Upper Oceanic Crust in the Eastern Equatorial Pacific: A Synthesis of Results from Site 504 (DSDP Legs 69, 70, and 83, and ODP Legs 111, 137, 140, and 148). , 0, , .		69
185	Data report: Low-grade hydrothermal alteration of uplifted lower oceanic crust, Hole 735B: mineralogy and isotope geochemistry. , 0, , .		6
186	Data Report: Microprobe Analyses of Primary Phases (Olivine, Pyroxene, and Spinel) and Alteration Products (Serpentine, Iowaite, Talc, Magnetite, and Sulfides) in Holes 1268A, 1272A, and 1274A. , 0, , .		11
187	CORK-Lite: Bringing Legacy Boreholes Back to Life. Scientific Drilling, 0, 14, 39-43.	0.6	11
188	IODP Expedition 336: initiation of long-term coupled microbiological, geochemical, and hydrological experimentation within the seafloor at North Pond, western flank of the Mid-Atlantic Ridge. Scientific Drilling, 0, 17, 13-18.	0.6	5
189	Time-lapse characterization of hydrothermal seawater and microbial interactions with basaltic tephra at Surtsey Volcano. Scientific Drilling, 0, 20, 51-58.	0.6	14
190	SUSTAIN drilling at Surtsey volcano, Iceland, tracks hydrothermal and microbiological interactions in basalt 50 years after eruption. Scientific Drilling, 0, 25, 35-46.	0.6	16
191	Design of the subsurface observatory at Surtsey volcano, Iceland. Scientific Drilling, 0, 25, 57-62.	0.6	3
192	IODP New Ventures in Exploring Scientific Targets (INVEST): Defining the New Goals of an International Drilling Program. Scientific Drilling, 0, 9, 54-64.	0.6	1
193	Data report: X-ray fluorescence scanning of sediment cores from Holes U1382B, U1383D, U1384A, and 1074A from the North Pond area. Proceedings of the Integrated Ocean Drilling Program Integrated Ocean Drilling Program, 1, .	1.0	1
194	Geochemistry of Hydrothermal Fluids From the E2-Segment of the East Scotia Ridge: Magmatic Input, Reaction Zone Processes, Fluid Mixing Regimes and Bioenergetic Landscapes. Frontiers in Marine Science, 0, 9, .	2.5	1